

Equilibrium Constants from Spectrophotometric Data: Dimer Formation in Gaseous Br₂

Joel Tellinghuisen*

Department of Chemistry, Vanderbilt University, Nashville, Tennessee 37235

Received: March 7, 2008; Revised Manuscript Received: April 14, 2008

The equilibrium constant for the dimerization reaction, $2\text{Br}_2(\text{g}) \rightleftharpoons \text{Br}_4(\text{g})$, is estimated using the classic spectrophotometric method with precise data and a multiwavelength fitting approach. The analysis is very sensitive to small errors in the data, requiring that parameters for the baseline absorption be included at each wavelength. To that end spectra for 18 Br₂ pressures in the range 6–119 Torr are augmented by six baseline scans to facilitate estimation of three baseline constants and two molar absorptivities at each wavelength, yielding $K_c = 2.5 \pm 0.4$ L/mol at 22 °C. This value is more than double the only previous estimate, which was based on analysis of PVT data. With adoption of a literature estimate of $\Delta H^\circ = -9.5$ kJ/mol, the new K implies $\Delta S^\circ = -51$ J mol⁻¹ K⁻¹ (ideal gas, 1 bar reference). The spectra for monomer absorption (peak 227 nm) and dimer absorption (205 nm) are obtained with unprecedented precision.

Introduction

The absorption spectrum of Br₂(g) displays a pressure-dependent band near 200 nm, as shown in Figure 1.^{1–4} The dependence of this band on pressure and temperature clearly indicates that the source is Br₂ dimers in equilibrium with monomers, with the dimerization reaction being characterized by $-\Delta H^\circ = 2.3$ – 2.6 kcal/mol.^{2,3} Because there is also a weak transition due to Br₂ in this spectral region, the spectrophotometric data at a given temperature T have been interpreted as a sum of contributions from the two species,^{3,4}

$$A_\lambda = b(\epsilon_{1\lambda}[\text{Br}_2] + \epsilon_{2\lambda}K_c[\text{Br}_2]^2) \quad (1a)$$

$$\approx b(\epsilon_{1\lambda}c + \epsilon_{2\lambda}K_c c^2) \quad (1b)$$

where A_λ is the absorbance at wavelength λ , b is the path length, K_c is the equilibrium constant in concentration units, and ϵ represents the molar absorptivity. In the approximate second version of eq 1, dimers are assumed to constitute a negligible fraction of the gas mixture, whence $c = P/RT$; analysis with this version can yield only the product $\epsilon_{2\lambda}K_c$, leaving the equilibrium constant unknown. Kokovin attempted to estimate this constant from PVT data for Br₂(g) in the 95–175 °C temperature range,^{5,6} obtaining a ΔH° value close to the spectrophotometry-based estimate and an extrapolated estimate of $K_c = 1.1$ L/mol at 25 °C. However, this analysis was based on a model in which all deviations from ideal gas behavior were attributed to dimer formation, with the system treated as an ideal gas mixture of Br₂ and Br₄. As Wen and Noyes noted,⁴ such an oversimplified model cannot be trusted to reliably handle real gas behavior under the conditions of Kokovin's experiments (up to 3.4 atm).

On the other hand, the spectrophotometric studies have typically been conducted at pressures of ~ 100 Torr or less and well below the condensation pressure, so the treatment of the system as an ideal gas mixture should be reliable for the interpretation of the absorption data. The primary purpose of the present study is to note that when eq 1 is implemented in its exact version for such a mixture, K_c can be estimated from

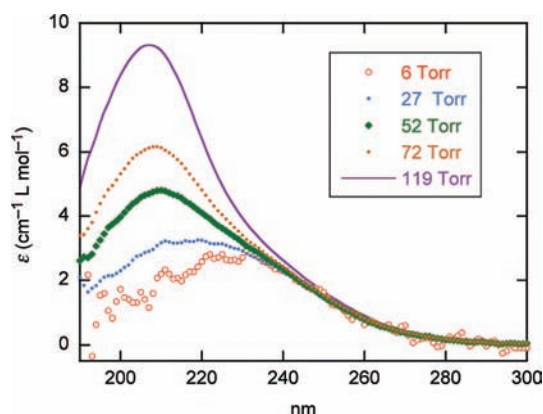


Figure 1. Apparent molar absorptivity for Br₂(g), as obtained from spectra recorded in a 9.71 cm silica cell at 22.3 °C and the indicated pressures.

high-quality spectrophotometric data, especially when data from multiple pressures and wavelengths are analyzed simultaneously. Here 18 spectra recorded at 1 nm intervals between 190 and 300 nm and pressures between 6 and 119 Torr are analyzed to yield an estimate of K_c more than double the value obtained by Kokovin, with an uncertainty estimated to be less than 20%.

It is true, however, that such an analysis is extremely demanding on the data. For example, although the instrumental baseline was zeroed at the outset of the experiments, the analysis indicated that deviations from zero, though typically less than 0.001 absorbance unit, were still statistically significant when included in the analysis model and led to significant changes in the resulting K_c estimates. This high sensitivity of the results to the data led me to examine the least-squares (LS) fitting problem with Monte Carlo computations, confirming that the LS fit results indeed represent a valid assessment of the parameters in this unusual situation.

Experimental Section

Data were obtained using equipment and procedures similar to those described in an earlier study of BrCl in Cl₂/Br₂ gas mixtures.⁷ Spectra were recorded between 190 and 300 nm at a resolution and interval of 1 nm on a Shimadzu UV-2101PC

* Corresponding author. Phone: (615) 322-4873. Fax: (615) 343-1234. E-mail: joel.tellinghuisen@vanderbilt.edu.

UV–visible spectrophotometer, using a 9.71 cm (± 0.02 cm) quartz cell equipped with Suprasil windows. No check was made of the photometric accuracy, which is stated as ± 0.004 at $A = 1$ by the manufacturer; for reference, the maximum recorded absorbance was ~ 0.6 . The cell was attached to a vacuum line (~ 1 mTorr minimum pressure; 1 Torr ≈ 133 Pa) for direct pressure measurement with a quartz bourdon gauge (Texas Instruments), which was calibrated against a mercury manometer. The sensitivity and precision of the pressure measurements was ~ 0.01 Torr, and the absolute accuracy (from the calibration) is estimated to be $\sim 0.1\%$ for $P > 10$ Torr. The experiments were conducted at ambient temperature, measured to be 22.3 ± 0.3 °C for the room but with no active control of the cell compartment in the spectrophotometer. Earlier checks indicated the latter could be as much as 3° warmer,⁷ so the true temperature is 22–25 °C. The T uncertainty does not manifest as fluctuations (see below) but does translate into a $\sim 1\%$ uncertainty in the derived K_c at the reported T of 22 °C.

Bromine (Fisher, reagent grade) was stored in a bulb on the vacuum system following trap-to-trap distillation at 0 °C and differential evaporation designed to minimize the more volatile (Cl₂) and less volatile (water) impurities. It was admitted to the cell at various pressures, after use of a discard portion to rinse the system. The ideal gas law was used to convert pressures to concentrations for the analysis of the absorption data, discussed further below.

As was noted earlier, the baseline becomes an important element in the analysis of the data. Although the baseline is zeroed at the outset via a standard instrumental function, it is not truly zero, as can be seen from the statistics from multiple baseline scans. Furthermore, the noise is frozen differently in the instrument each time the baseline function is run, which becomes a problem when data from experiments run with different instrumental parameter settings are combined for analysis. In the present case, the 18 original spectra were augmented by six baseline scans covering the three different settings of the instrument parameters for the spectra in question and were analyzed as described below.

Analysis

Letting 1 and 2 refer to monomeric and dimeric Br₂, an ideal gas mixture of the two yields for the concentrations, $c = c_1 + c_2$, with $c = P/RT$ and P the measured pressure. Because $c_2 = K_c c_1^2$, substitution and solution for c_1 yields

$$c_1 = (2K_c)^{-1} [(1 + 4K_c c)^{1/2} - 1] \quad (2)$$

Use of this expression for [Br₂] in eq 1a permits estimation of ϵ_1 , ϵ_2 , and K_c from data at a single wavelength in favorable circumstances. In less favorable circumstances, data from multiple wavelengths can be fitted to a single K_c and two ϵ values at each wavelength. As mentioned earlier, it is also necessary to include extra constants at each wavelength to allow for nonzero baseline levels; in the final analysis, three such parameters were included, covering the three settings of the instrumental parameters and the baseline function, with two baseline scans representing each set of spectra and treated as zero-concentration spectra. Thus in this analysis the 24 A_λ values at each wavelength were represented by five adjustable parameters, plus a single value of K_c for all wavelengths.

From the LS standpoint, estimation of K_c from such data rests entirely on subtle differences in the shapes of the A vs c curves for the data as predicted from the exact and approximate versions of eq 1. Thus, as the fractional dimerization becomes small, the differences between c and c_1 become too small to permit

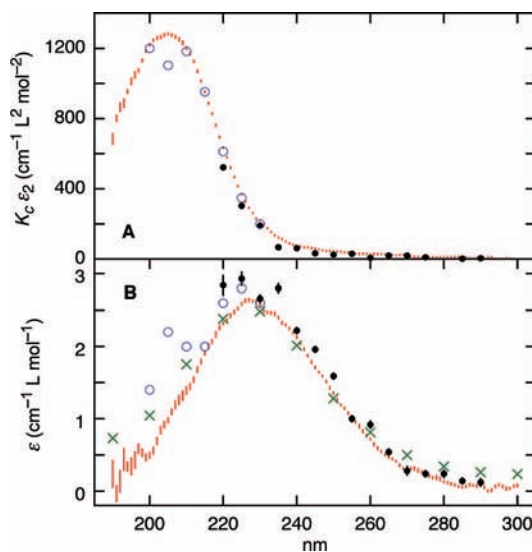


Figure 2. Results for dimer (A) and monomer (B) absorption in Br₂(g) from quadratic analysis of 18 absorption spectra recorded at pressures from 6 to 119 Torr and room T (vertical lines representing $\pm 1\sigma$). The analysis employed a single baseline parameter A_0 . Points represent estimates from refs 3 (open) 4, (solid), and 9 (\times).

such an estimation. Early computations on data at a wavelength near the peak in the dimer absorption spectrum indicated that such an analysis might be barely feasible for data at a single wavelength, with apparent σ_{K_c} values somewhat smaller than K_c itself. Then simultaneous analysis of data at N wavelengths would be expected to reduce σ_{K_c} by roughly the factor $N^{-1/2}$ for wavelengths where the information content in the data is comparable. To better understand the subtleties in this problem and to ensure that the LS parameter error estimates are realistic, I conducted Monte Carlo (MC) computations on a model designed to replicate the experimental data at the selected wavelength. Both the LS computations and their MC implementation employed methods like those described earlier in this journal.⁸

Results and Discussion

Preliminary Analysis. Figure 2 shows results from a wavelength-by-wavelength analysis of the 18 “real” spectra by eq 1b, with earlier results included for comparison. The new analysis shows good agreement with the earlier results for the dimer absorption but makes the monomer absorption somewhat weaker. This analysis also yields valuable information for the estimated data error, shown in Figure 3. An earlier effort to characterize the error for this instrument did not cover this wavelength region very well,¹⁰ though it did indicate that the dependence on A should be small for the $A = 0$ – 0.6 range spanned by the present data. This means that weighting is not needed for single- λ analysis via eq 1. However, the strong λ dependence evident in Figure 3 implies that weights are important in a multiwavelength analysis of data that span a significant wavelength range. The fitted curve in Figure 3 was obtained from an unweighted fit of the logarithmic sampling estimates of the variance; this is appropriate, because variance estimates themselves have proportional error, making the error in $\ln(s^2)$ constant.¹¹

Figure 4 shows the data at 205 nm fitted to both versions of eq 1. The two fitted functions are indistinguishable without expanding the scale, after which they are seen to extrapolate differently to zero concentration, even though the data span all

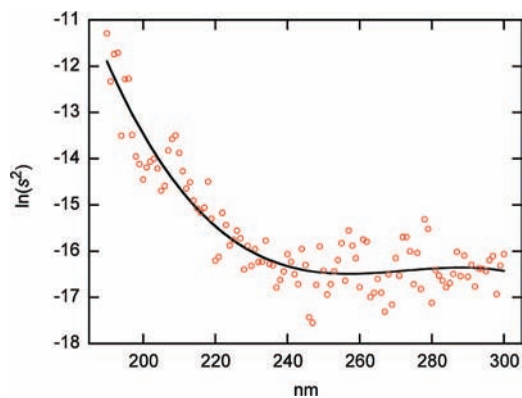


Figure 3. Sampling estimates of data variance from quadratic analysis of Figure 2, displayed logarithmically. The solid curve displays the fitted function, of form $\ln(s^2) = -16.49 + 0.00042(\lambda - 257)^2 - 9 \times 10^{-6}(\lambda - 257)^3$.

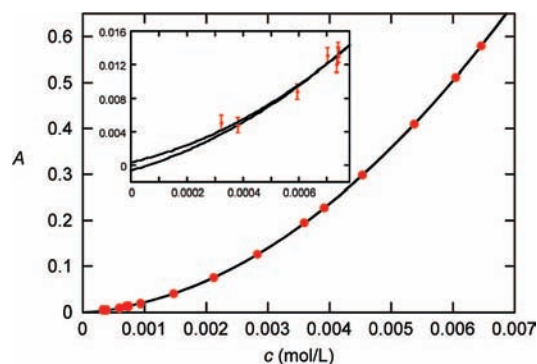


Figure 4. Absorbance as a function of Br_2 concentration at 205 nm, with curves showing results of fitting to eq 1 and to its modified form incorporating K_c via eq 2. The difference in the two fits is shown at expanded scale near the origin in the inset. The unweighted three- and four-parameter fits yield, for ϵ_1 , 0.98(3) and 0.79(9) $\text{cm}^{-1} \text{L mol}^{-1}$, respectively, and for $K_c \epsilon_2$, 1282(5) and 1358(36) $\text{cm}^{-1} \text{L}^2 \text{mol}^{-2}$, respectively. The four-parameter fit yields $K_c = 2.9 \pm 1.3 \text{ L mol}^{-1}$. The estimated standard deviations in A are 0.00064 and 0.00057, respectively.

but the first 5% of the concentration range. This observation led to increased concern about the role of the zero level (A_0) in the analysis and raised the question whether this parameter could or should be fixed in the analysis. These concerns were further heightened by the initial global fits, run over just the 190–240 nm region where the dimer absorption is prominent: Including an adjustable parameter for A_0 at each wavelength led to an estimate of $K_c = 3.2(6) \text{ L/mol}$, and freezing all A_0 at 0.0 yielded 1.8(2). This much difference was surprising, given that the fitted A_0 values were mostly less than 0.001 in absolute value. This matter of the baseline and its proper treatment is addressed in more detail below.

Monte Carlo Calculations. The high sensitivity of the single-wavelength fits to A_0 , and the resulting large uncertainties in K_c raised concerns about the reliability of the nonlinear LS fit model. Especially important is the question, is it possible to get apparent K_c estimates from use of the four-parameter model on data that could be fitted just as well with the three-parameter model? To address these concerns, I conducted MC computations on models replicating the data shown in Figure 4. Specifically, true functions of both forms were assumed and were then analyzed by both fit models, using 10^5 replicate data sets in each case to generate the MC statistics. The data error was assumed to be 0.0006, independent of A . The key results may be summarized as follows:

- The four-parameter fit to eq 1a is nonlinear, so the parameter estimates are not normally distributed.⁸ However, A_0 , ϵ_1 , and K_c are quite close to normal, even for the large uncertainty in the last of these. On the other hand, ϵ_2 is grossly abnormal, which can be seen by recalling that the product $K_c \epsilon_2$ is rigorously normal in the three-parameter fit to eq 1b (which is linear), making ϵ_2 the ratio of a fairly precise normal variate ($K_c \epsilon_2$) and an imprecise one (K_c). This gives ϵ_2 the pathological properties of a reciprocal variate.^{8,12} From a practical standpoint it means that the nonlinear LS fits are better conducted with the adjustable parameters defined as K_c and $K_c \epsilon_2$ than as K_c and ϵ_2 . Indeed, the latter choice led to divergence in most of the MC data sets, and the former gave 100% convergence. A similar behavior has been noted in the analysis of isothermal titration calorimetric data.¹³
- The estimates of K_c are biased by about +0.03 L/mol, and the error estimates are valid within a few percent. The standard error in K_c drops from about 1.5 L/mol at $K_c = 3.2 \text{ L/mol}$ to 1.3 at 0.0, so K_c becomes statistically undefined (from the standpoint of ad hoc fitting) around $K_c = 1.4 \text{ L/mol}$. Of course these results apply for a single 18-point data set, so the error will narrow roughly as $N^{-1/2}$ when N comparable data sets are included in a global analysis.
- When data generated with the exact four-parameter model are fitted to eq 1b, the estimate of ϵ_1 is 25% too large and $K_c \epsilon_2$ is 6% low, and the sum of squared residuals (equivalent to χ^2) is 33% larger. These relations are roughly as observed in the prototype data set of Figure 4.
- When data are generated with eq 1b and fitted with the four-parameter model, the estimates for A_0 , ϵ_1 , and $K_c \epsilon_2$ are all approximately correct, though more uncertain than when fitted with the three-parameter model, as expected. The estimate of K_c is $0.03 \pm 1.4 \text{ L/mol}$, and there is no appreciable change in χ^2 .

In short, the observation of successful fitting of data like those in Figure 4 to the four-parameter model including K_c is solid evidence that this quantity is indeed determined.

The Baseline. Commercial double-beam spectrophotometers like the instrument used here typically have a baseline function that the operator runs at the outset to zero the sample cell against an identical reference cell. For routine work it then suffices to treat the measured sample A values as absolute. However, the present application is not routine, and the demands on the data require a more careful treatment of the baseline. In particular, the baseline function freezes systematic error into the zero level, but at such a low level that it is not evident for a single blank spectral scan.

This point is illustrated in Figure 5, where average results of three sets of ten baseline scans are shown. The first two sets were recorded for the same baseline function and exhibit considerably more mutual similarity than either of these does with the third. The error is always less than 0.001 in magnitude for $\lambda > 220 \text{ nm}$ but increases sharply below 200 nm, where the intensity of light transmitted through the system drops.

The role of systematic error in the baseline was not fully appreciated at the time the Br_2 absorption spectra were recorded, so no great effort was made to characterize the baseline function. However, two baseline spectra were recorded for each of the three baseline functions employed in those experiments. In the final LS analysis, these six baseline scans were just included as zero-concentration spectra, as has already been noted.

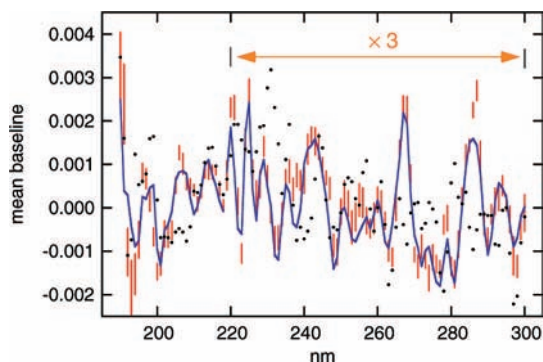


Figure 5. Average baselines from three sets of 10 spectra. The first two sets (vertical bars and solid line) were recorded about an hour apart, for the same baseline function; the third (points) were recorded after resetting the baseline. The vertical bars represent the standard error for the first set (comparable for the others). Note the scale expansion for $\lambda > 220$ nm.

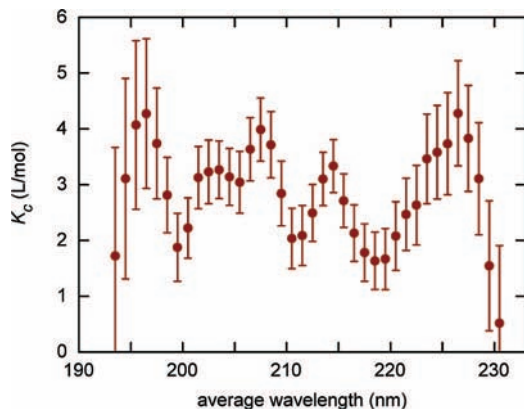


Figure 6. Estimated K_c values and standard errors from analysis of data at four adjacent (1 nm) wavelengths in the region of strong dimer absorption, shown as a function of the average wavelength.

Global Analysis. The data were first analyzed for small numbers of wavelengths in the wavelength region of prominent dimer absorption to check for possible systematic effects. The results (Figure 6) show variability but no particular trend. When all data in the 190–235 nm region are analyzed together, the result is $K_c = 2.70(21)$ L/mol. Expansion of the data set to include data beyond 235 nm reduces the value somewhat (~ 2.6 L/mol), and successive deletion of short-wavelength data leads to further decrease—to 2.4 L/mol when all data below 205 nm (the peak in the dimer spectrum) are omitted, for example. The all-data estimate is $K_c = 2.52(28)$ —a value that well encompasses the results from the selected data subsets.

Although the use of three constant parameters at each wavelength is justified, it actually has little effect on the resulting K_c values. For example when just the 11 high- P spectra and their two baselines are analyzed at all wavelengths, the result is $K_c = 2.64(31)$ L/mol. Addition of one set of 5 low- P spectra and their two baselines, with an additional baseline parameter, gives 2.38(29) L/mol. Adding the remaining 4 low- P spectra and two baseline spectra, still with two baseline parameters, gives 2.48(28) L/mol. On the other hand, analyzing all spectra with a single baseline parameter gives 2.20(28) L/mol.

Although the spectrophotometer cell compartment was not thermostatted, leading to the aforementioned ~ 2 K uncertainty in the actual cell temperature, there was no indication of spectrum-to-spectrum temperature fluctuations on this scale. To check on this, I modified the fit model to incorporate concentration correction parameters for selected spectra. When applied

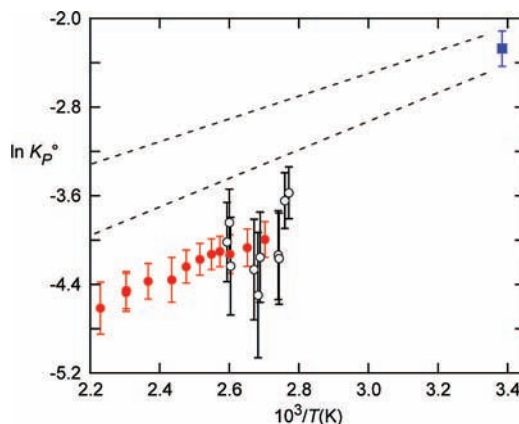


Figure 7. Van't Hoff plot comparing present estimate of K_P° (square) with estimates from analysis of PVT data from ref 5 (open) and ref 6 (solid). The dashed lines represent the broadest extrapolation of the present results using $\Delta H^\circ = -2.27(25)$ kcal/mol from ref 3. Errors bars on the PVT results have been generated from information provided in those works.

to the highest- P spectrum (119 Torr), this factor was 1.00020 and led to an increase in K_c by 0.17 L/mol. The last four low- P spectra were recorded 5 h after the others and gave 0.9996 for this factor (applied to all), and a smaller rise in K_c . At the other extreme, five spectra recorded at pressures 130–180 Torr in an intermediate time period, and not included in the final data set, *could* be included by this tactic. All showed correction factors very close to 0.990 and gave K_c values dropping as low as 1.87 and then rising to 2.96 L/mol, as they were successively added to the data set. This behavior again illustrates the high sensitivity of the analysis of K_c to the data.

From considerations such as these, I conclude that the value 2.5(4) L/mol is a reasonable assessment of the results, with allowance for data selection and model dependence in the analysis. This converts to a K_P value of 0.103 atm⁻¹ (0.104 bar⁻¹); and in the assumption of T -independent ΔH° and ΔS° , use of $\Delta H^\circ = -2.27(25)$ kcal/mol (-9.5 ± 1.0 kJ/mol)³ yields $\Delta S^\circ = -12.2(9)$ cal mol⁻¹ K⁻¹ (-51 ± 4 J mol⁻¹ K⁻¹).

The new value (converted to K_P°) is compared with the previous PVT -based estimates in Figure 7, using the spectrophotometry-based estimate of ΔH° to predict the extension of the present value to higher T . As was noted earlier, the discrepancy is about a factor of 2. A treatment of PVT data in terms of a mixture of monomers and dimers, both treated as ideal, should indeed lead to a discrepancy in this direction. For example, the van der Waals equation can be expressed

$$P = \frac{cRT}{1 - bc} - ac^2 \quad (3)$$

From the standpoint of this equation, the model employed by Kokovin is tantamount to equating a with RTK_c and neglecting b . But the excluded volume effects represented by b would not be negligible at the pressures employed in the PVT studies, so a more realistic first correction term is $(bRT - a)c^2$. A virial-equation treatment also yields this result for the first correction term.¹⁴ The effect of the b term is to raise the PVT estimate of a , but not by enough to account for the discrepancy, because a reasonable estimate for b in dilute gases is 4 times the molecular volume, or about 0.2 L/mol for Br₂. Indeed, when the PVT data from refs 5 and 6 are fitted to expressions like eq 3, both with and without an extra virial-like term in c^3 , with a incorporating a T -dependent K_P (for constant ΔH° , fixed at -2.27 kcal/mol), the largest increase in the extrapolated Kokovin K_P is only

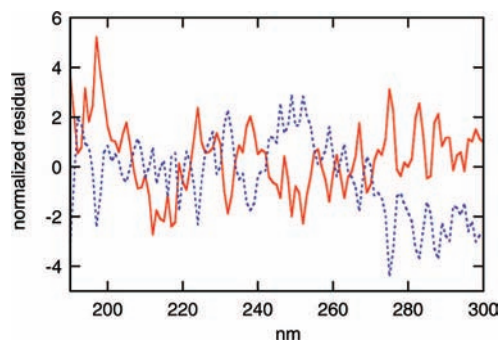


Figure 8. Normalized residuals from fits of the monomer (solid) and dimer (dashed) molar absorptivities to the functions given in eqs 4 and 5, respectively. The plotted quantities represent the LS estimated values of ϵ minus the fitted band function, divided by the LS estimated σ_ϵ . The ϵ values were obtained by fitting with $K_c = 2.5$ L/mol; residual uncertainties for the dimer do not include that in K_c . The band parameters for the monomer are (units nm and L mol⁻¹ cm⁻¹): $a = 1.231$, $b = 19.85$, $\lambda_0 = 230.1$, $c = 120$. For the dimer: $a = 431$, $\lambda_1 = 202.3$, $b = 28.4$, $c = 160$, $\lambda_2 = 212.7$, $d = 13.1$.

~50%. Thus this discrepancy remains unresolved. The treatment of the absorption data by the model of eqs 1 and 2 does not suffer from such problems, and at the highest P of the present data the dimer pressure is calculated to be 1.6% of the monomer pressure.

In an analogous spectrophotometric treatment of gas-phase dimerization in I₂, conducted at much higher temperatures and pressures than the present experiments, Passchier and Gregory obtained results that extrapolated to a reported $K_c = 1.7$ L/mol at room T .¹⁴ However, a consistent extrapolation of their results at 605 K yields 2.4 ± 1.0 L/mol at 25 °C. Their estimated $-\Delta H^\circ$ for I₂ dimerization was about 25% larger than their value for Br₂, at 2.9(4) kcal/mol; similarly, $-\Delta S^\circ$ is somewhat larger for I₂, at 14.4 cal mol⁻¹ K⁻¹. Ab initio computations on Br₄ have not yet succeeded in accounting for such large dimer bond energies.¹⁵

The final spectra differ little from those shown in Figure 2. They are available in numerical form in the Supporting Information, along with the raw spectrophotometric data. Both bands can be fairly well represented by simple band functions: a modified log-normal^{16,17} for the monomer,

$$f_{\text{mon}}(\lambda) = \frac{a}{1 - c/\lambda} \exp[-b(\ln(X))^2]; \quad X = \frac{\lambda - c}{\lambda_0 - c} \quad (4)$$

and a sum of a Gaussian and a Lorentzian for the dimer,

$$f_{\text{dim}}(\lambda) = a \exp[-4 \ln(2)(\lambda - \lambda_1)^2/b^2] + \frac{c}{1 + (\lambda - \lambda_2)^2/d^2} \quad (5)$$

with the Lorentzian needed to reproduce the long-wavelength tail. The parameters for the two bands are given in the caption to Figure 8, which shows the residuals from these representations. Although there appears to be statistically significant structure in both bands, the residuals are highly correlated and the structure is just an artifact of this correlation. Both bands are poorly represented at their short-wavelength end, but the statistical errors are also larger there, from attenuated instrumental source radiation in this region.

The monomeric band is a factor of 4 weaker at its peak than the weakest of the three well-known bands at longer wavelength ($A \leftarrow X$)¹⁸ and has long been interpreted as the analog of the 270 nm band in I₂, which involves absorption to an unbound

I_u state of ion-pair character.^{19–21} This symmetry has been confirmed through photofragment imaging studies, but with an indication of a minor contribution from parallel ($\Delta\Omega = 0$) transitions on the long-wavelength side.^{22–24} A recent ab initio treatment predicts this band to be 30% narrower than observed and about a factor of 2 weaker overall.²⁵

From the earliest observation of pressure-dependent absorptions in the halogens, the phenomena have been attributed to charge-transfer transitions involving either bound dimers or collision complexes.²⁶ The observation of significantly negative ΔH° from the T dependence of the dimer bands demonstrates clearly that bound dimers predominate in the absorption.² Little specific information has been offered about these transitions, and this study cannot change that. Both the monomer and dimer bands are about a factor of 5 weaker in bromine than in iodine.

Conclusion

Precise spectrophotometric data for absorption by gaseous bromine in the 190–300 nm region are analyzed by a multi-wavelength least-squares technique to yield an estimate of 2.5(4) L/mol for the dimerization equilibrium constant at 295 K. This value exceeds by more than a factor of 2 the only other estimate, provided long ago from analysis of *PVT* data. On the other hand, it and its related thermodynamic properties are commensurate with values obtained for the analogous process in gaseous iodine.

Under the conditions of the present experiments, the maximum conversion to dimers is <2%. However, the dimers in both Br₂ and I₂ appear to be strongly enough bound to make them prominent or even dominant at the low effective temperatures achieved in free-jet expansions, as have been employed in many studies of weak interactions between halogens and other molecules.^{27,28} I am unaware of any such attempts specifically targeting the UV dimer absorption.

An important aside from this study is the need to pay attention to the baseline in such demanding spectrophotometric work. It is easy to demonstrate the existence of statistically significant systematic error in the baseline function for the instrument used in the present study; it seems likely that other instruments will be found to behave similarly.

Supporting Information Available: Table 1S includes all of the spectral data used in the analysis, and Table 2S gives the resulting values of ϵ_1 , ϵ_2 , and the three background parameters at each wavelength. This material is available free of charge via the Internet at <http://pubs.acs.org>.

References and Notes

- (1) Evans, D. F. *J. Chem. Phys.* **1955**, *23*, 1426.
- (2) Ogryzlo, E. A.; Sanctuary, B. C. *J. Phys. Chem.* **1965**, *69*, 4422.
- (3) Passchier, A. A.; Christian, J. D.; Gregory, N. W. *J. Phys. Chem.* **1967**, *71*, 937.
- (4) Wen, W. Y.; Noyes, R. M. *J. Phys. Chem.* **1972**, *76*, 1017.
- (5) Lasater, J. A.; Colley, S. D.; Anderson, R. C. *J. Am. Chem. Soc.* **1950**, *72*, 1845.
- (6) Kokovin, G. A. *Russ. J. Inorg. Chem.* **1965**, *10*, 150.
- (7) Tellinghuisen, J. *J. Phys. Chem. A* **2003**, *107*, 753.
- (8) Tellinghuisen, J. *J. Phys. Chem. A* **2000**, *104*, 2834.
- (9) Hubinger, S.; Nee, J. B. *J. Photochem Photobiol. A* **1995**, *86*, 1.
- (10) Tellinghuisen, J. *Appl. Spectrosc.* **2000**, *54*, 431.
- (11) Tellinghuisen, J. *Analyst* **2008**, *133*, 161.
- (12) Tellinghuisen, J. *J. Phys. Chem. A* **2000**, *104*, 11829.
- (13) Tellinghuisen, J. *J. Phys. Chem. B* **2005**, *109*, 20027.
- (14) Passchier, A. A.; Gregory, N. W. *J. Phys. Chem.* **1968**, *72*, 2697.
- (15) Schuster, P.; Mikosch, H.; Bauer, G. *J. Chem. Phys.* **1998**, *109*, 1833.
- (16) Maric, D.; Burrows, J. P. *J. Phys. Chem.* **1996**, *100*, 8645.
- (17) Tellinghuisen, J. *J. Phys. Chem. A* **2001**, *105*, 11183.
- (18) (a) Tellinghuisen, J. *J. Chem. Phys.* **2001**, *115*, 10417. (b) Tellinghuisen, J. *J. Chem. Phys.* **2003**, *118*, 1573.

- (19) Mulliken, R. S. *J. Chem. Phys.* **1971**, 55, 288.
- (20) Clear, R. D.; Wilson, K. R. *J. Mol. Spectrosc.* **1973**, 47, 39.
- (21) Hwang, H. J.; El-Sayed, M. A. *J. Phys. Chem.* **1991**, 95, 8044.
- (22) Jee, Y.-J.; Park, M. S.; Kim, Y. S.; Jung, Y.-J.; Jung, K.-H. *Chem. Phys. Lett.* **1998**, 287, 701.
- (23) Cooper, M. J.; Wrede, E.; Orr-Ewing, A. J.; Ashfold, M. N. R. *J. Chem. Soc., Faraday Trans.* **1998**, 94, 2901.
- (24) Jee, Y.-J.; Jung, Y.-J.; Jung, K.-H. *J. Chem. Phys.* **2001**, 115, 9739.
- (25) Asano, Y.; Yabushita, S. *Chem. Phys. Lett.* **2003**, 372, 348.
- (26) Tamres, M.; Strong, R. L. In *Molecular Association*; Foster, R., Ed.; Academic Press: London, 1979; Vol. 2, p 331.
- (27) Fei, S.; Zheng, X.; Heaven, M. C.; Tellinghuisen, J. *J. Chem. Phys.* **1992**, 97, 6057.
- (28) Zhong, D.; Bernhardt, T. M.; Zewail, A. H. *J. Phys. Chem. A* **1999**, 103, 10093.
- (29) Tellinghuisen, J. *Appl. Spectrosc.* **2000**, 54, 1208 .

JP8020358